Spectroscopic Techniques: Lasers

44

Paul Engelking

Contents

44.1 **Laser Basics** . . . 649
44.1.1 Stimulated Emission . . . 649
44.1.2 Laser Configurations . . . 649
44.1.3 Gain . . . 650
44.1.4 Laser Light . . . 650

44.2 **Laser Designs** . . . 651
44.2.1 Cavities . . . 651
44.2.2 Pumping . . . 652

44.3 **Interaction of Laser Light with Matter** . . . 652
44.3.1 Linear Absorption . . . 652
44.3.2 Multiphoton Absorption . . . 654
44.3.3 Level Shifts . . . 654
44.3.4 Hole Burning . . . 654
44.3.5 Nonlinear Optics . . . 655
44.3.6 Raman Scattering . . . 655

44.4 **Recent Developments** . . . 656

References . . . 656

Abstract

As a primary research tool, the laser plays a fundamental role in the spectroscopic study of atomic and molecular systems. This Chapter describes the basic operating principles, configurations, and characteristic parameters of lasers. Laser designs are discussed and then the details of the interaction of the laser light with matter delineated. The reader is also referred to other chapters in the book for further information on laser principles and types of lasers.

Keywords

optical parametric oscillator · gain medium · integrated cross section · frequency comb · hole burning

P. Engelking (✉)
Dept. of Chemistry and Chemical Physics Institute, University of Oregon
Eugene, OR, USA

44.1 Laser Basics

44.1.1 Stimulated Emission

A cross section σ_{21} for absorption of radiation by a lower state 1 engenders a balancing cross section σ_{12} for emission stimulated by radiation interacting with an upper state 2. Detailed balance relates these two cross sections according to

$$g_2\sigma_{12} = g_1\sigma_{21} \,, \tag{44.1}$$

where g_1 and g_2 are the statistical degeneracies of their respective states [1].

For a collection of emitting and absorbing states with densities n_2 and n_1, amplification may occur when $n_2\sigma_{12} > n_1\sigma_{21}$, which leads to a requirement for an *inversion* of the state populations

$$n_2/n_1 > g_2/g_1 \,. \tag{44.2}$$

The rate of spontaneous emission at frequency ν can be modeled itself by stimulated emission induced by a noise source of the magnitude of the density of states $\rho(\nu)$

$$\gamma_{12}(\nu) = \sigma_{12}(\nu)\rho(\nu)/c = \sigma_{12}(\nu)8\pi\lambda^{-2} \,. \tag{44.3}$$

44.1.2 Laser Configurations

A practical laser combines a population inversion with a means for controlling the radiation.

The basic laser source is the laser oscillator, an amplifier possessing positive feedback. The usual form is simply a piece of active gain medium placed inside a resonant optical cavity (Fig. 44.1). Tunability is produced if the resonant cavity is frequency selective and adjustable (Fig. 44.2). Many laser sources use an amplifier after the oscillator.

G.W.F. Drake (Ed.), *Springer Handbook of Atomic, Molecular, and Optical Physics*, Springer Handbooks,
https://doi.org/10.1007/978-3-030-73893-8_44

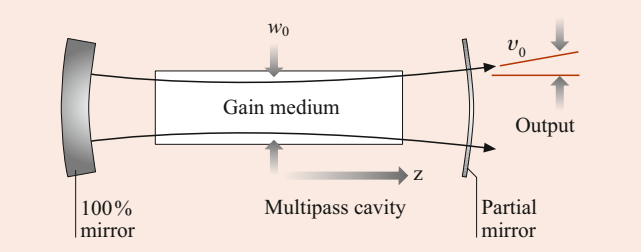

Fig. 44.1 Simple laser oscillator and beam parameters. Distances z are generally measured from the minimum beam waist w_0. The beam appears with a far-field divergence angle θ_0

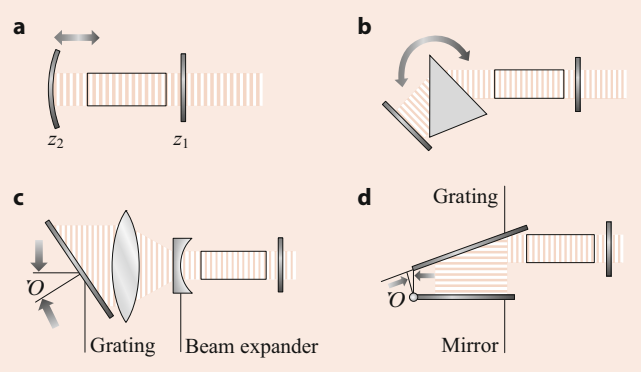

Fig. 44.2 Tunable laser oscillator geometries. **a** Fabry–Perot: tuning is usually done by changing the cavity length, although changing the index of refraction by changing the temperature or current is common with solid state laser diodes. **b** Littrow prism line selector: typical of atomic ion lasers capable of multiple line output. **c** Littrow grating tuning: common in pulsed dye lasers with high gain (> 10) per pass. Telescope increases resolution by filling, and reducing angular divergence at the grating. **d** Grazing incidence, mirror tuned, grating mount

44.1.3 Gain

The fundamental gain per pass is given by

$$G = J/J_0 = \exp[(\kappa - \mu)L] \,, \tag{44.4}$$

where J/J_0 is the ratio of light output to input, κ is the gain coefficient, μ is the nonradiative loss rate, and L is the path length. The gain coefficient

$$\kappa = n^* \sigma_{12} \tag{44.5}$$

depends upon the net inversion n^*,

$$n^* = n_2 - (g_1/g_2)n_1 \,. \tag{44.6}$$

If λ is the wavelength of radiation, F_{12} is the emission line shape function normalized over frequency ν, τ_2 is the lifetime of the transition, and f_{12} is the branching ratio for the upper state to undergo this transition, then the stimulated emission cross section is

$$\sigma_{12} = \frac{\lambda^2 f_{12} F_{12}(\nu)}{8\pi\tau_2} \,. \tag{44.7}$$

For a Lorentzian lifetime-broadened line, the cross section for stimulated emission at the line center becomes

$$\sigma_{12} = \frac{\lambda^2 f_{12}}{4\pi^2 \Gamma_{12}\tau_2} \,, \tag{44.8}$$

where Γ_{12} is the full width at half maximum of the line.

44.1.4 Laser Light

Lasers are inherently bright sources of radiation: the radiation field within a practical laser must be high enough for stimulated emission to compete with spontaneous emission. The effective source of spontaneous fluctuations approximates that of the density of states. In terms of the beam parameters photon flux J per solid angle Ω, and frequency ν, this is

$$\frac{\mathrm{d}^2 J}{\mathrm{d}\Omega \mathrm{d}\nu} = \frac{2\nu^2}{\epsilon_r c^2} \,. \tag{44.9}$$

Beam *quality* is given by the product of the angular divergence times the beam width. Highest beam quality is associated with diffraction limited light emitted from a Gaussian spot. For circular laser beams traveling in the z-direction, this corresponds to a solution of the electromagnetic wave equation

$$u(r, \phi, z) = \psi(r, z) \exp(-\mathrm{i}kz) \,, \tag{44.10}$$

where u is a polarization component of the field. For high values of $k = 2\pi/\lambda$, corresponding to short wavelength, the adiabatic radial solution is also Gaussian

$$\psi(r, z) = \exp\{-\mathrm{i}[P + kr^2/(2q)]\} \,, \tag{44.11}$$

where the complex phase shift P, beam parameter q, and beam radius w are functions of z

$$\begin{aligned} P(z) &= -\mathrm{i}\ln\left[1 - \mathrm{i}\frac{\lambda z}{\pi w_0^2}\right] \\ &= -\mathrm{i}\ln\sqrt{1 + \left[\frac{\lambda z}{\pi w_0^2}\right]^2} - \tan^{-1}\left[\frac{\lambda z}{\pi w_0^2}\right] \,, \end{aligned} \tag{44.12}$$

$$q(z) = \mathrm{i}\pi w_0^2/\lambda + z \,, \tag{44.13}$$

$$w^2(z) = w_0^2\left[1 + \left(\frac{\lambda z}{\pi w_0^2}\right)^2\right] . \tag{44.14}$$

Here, w_0 is the beam waist parameter, the minimum width of the Gaussian beam at a focused spot. For Gaussian beams, the product of the minimum beam waist and beam divergence angle θ_0 is given by

$$\theta_0 w_0 = \lambda/\pi \ . \tag{44.15}$$

The beam waist and divergence follow optical imaging according to paraxial ray theory.

Higher order circular modes with p radial nodes and l angular node planes are specified by multiplying Eqs. (44.11) and (44.12) by angular and radial factors to obtain

$$\psi_{pl}(r,\phi,z) = \left(\sqrt{2}r/w\right)^l L_p^l\left(2r^2/w^2\right) \mathrm{e}^{\mathrm{i}l\phi}\psi(r,z) \ , \tag{44.16}$$

$$P_{pl}(z) = (2p + l + 1)P(z) \ . \tag{44.17}$$

Here, the functions $L_p^l(x)$ are the Laguerre polynomials as defined in Sect. 9.4.2. The radial phase shifts produce a wave front curvature of effective radius

$$R = z + \left[(2p + l + 1)/2 + w_0^2\pi/\lambda^2\right]w_0^2\pi/z \ . \tag{44.18}$$

Modes with the same values of $2p + l$ have identical axial and radial phase shifts. The two polarization components of the electromagnetic field double the degeneracies of all modes considered here. Often these degeneracies are split in practice by optical inhomogeneities of the medium through which they pass. More details can be found in the summary of *Kogelnick* and *Li* [2], or in the texts by *Verdeyen* [3] or *Svelto* [4].

Some applications require knowledge of the electric field in additionto the flux density J. For purely sinusoidal single mode beams, the rms field is

$$\langle E\rangle = \left(\frac{h\nu J}{c\epsilon_0}\right)^{1/2} \ . \tag{44.19}$$

Nonlinear effects are often expressed in terms of powers of the field by

$$\langle E^n\rangle = 2^{(n-1)/2}\langle E\rangle^n \tag{44.20}$$

for single mode and multimode radiation of random frequency spacings. For m equally spaced modes, this is increased by $m!/(m-n)!$.

44.2 Laser Designs

44.2.1 Cavities

The simple Fabry–Perot cavity consists of two spherical mirrors facing one another. The surfaces are chosen to be constant phase surfaces for the desired modes in Eq. (44.18).

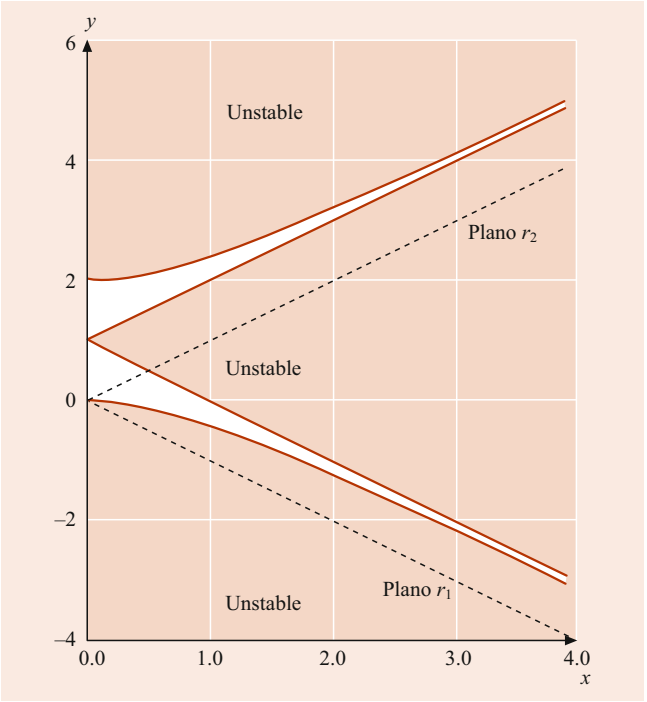

Fig. 44.3 Stability parameters for simple two-mirror laser cavities of length L and mirror radii of curvature R_1 and R_2. Here, $x = \frac{1}{2}(L/R_1 - L/R_2)$ is the mean curvature difference of the two mirrors; $y = \frac{1}{2}(L/R_1 + L/R_2)$ is the mean curvature of the two mirrors. Cavities with parameters in the unshaded region are stable

Stability criteria are shown in Fig. 44.3. A cavity is stable when initial angles θ and displacements r of paraxial rays transform during a round trip into θ' and r' satisfying

$$-2 < \frac{\partial\theta'}{\partial\theta} + \frac{\partial r'}{\partial r} < 2 \ . \tag{44.21}$$

At frequencies for which the round-trip phase change per passage

$$\begin{aligned}\delta(\nu) &= 2\pi(z_2 - z_1)\nu/c + 2\left[P_{pl}(z_2) - P_{pl}(z_1)\right] \\ &\approx 2\pi(z_2 - z_1)/\lambda + \pi(2p + l + 1)\end{aligned} \tag{44.22}$$

is an integer multiple of 2π, the phases from different passages interfere constructively, giving longitudinal modes. (Here $P_{pl}(z_i)$ gives the additional phase shift for higher transverse modes at mirrors $i = 1, 2$.)

For a particular radial mode structure in an empty Fabry–Perot cavity, the ratio of the maximum cavity decay time for these standing waves to the minimum cavity decay time for frequencies between longitudinal modes is

$$(1 + r)^2/(1 - r)^2 \ . \tag{44.23}$$

Here r is the reflectivity of the end mirrors; for cavities with mirrors having different reflectivities, one may use the square

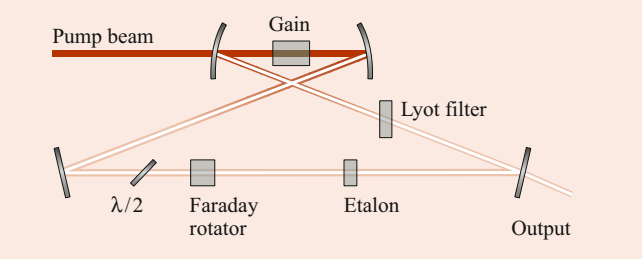

Fig. 44.4 Ring laser. The Faraday rotator and half-wave plate permit circulation of the cavity fields in only one direction

root of the product of their reflectivities. A simple Fabry–Perot cavity may be tuned by changing the cavity length or by changing the index of refraction of the cavity material. Since both of these may be properties of temperature, temperature tuning may be possible. The index of refraction of a material may also be sensitive to the intensity of excitation. Diode lasers consisting of a semiconductor die with polished, reflecting faces are often tuned by changing temperature and pumping current.

For lasers with a dispersive optical element within the cavity, highest selectivity is obtained when the light has low angular divergence and impinges upon the dispersive element as nearly plane waves. A beam expander may reduce the angular spread while simultaneously increasing the beam width. For a grating used as a mirror in a Littrow mount, the dispersion equation is

$$\Delta\lambda = (d/n)\cos\phi\,\Delta\phi\ , \tag{44.24}$$

where n is the diffraction order, d is the distance between lines, and ϕ is the angle of incidence off normal.

Cavities with prisms or gratings can be conveniently tuned by rotating the angle of the dispersive element. For a grating used as a mirror in a Littrow mount, the grating equation is

$$\lambda = (2d/n)\sin\phi\ . \tag{44.25}$$

Often, more than one longitudinal cavity mode operates within the selected frequency band, and tuning consists of *hopping* from mode to mode, rather than smoothly sweeping a single line across a band of frequencies. Smooth frequency tuning can be achieved, for example, in a design by *Wallenstein* and *Hänsch* [5], in which the grating and Fabry–Perot cavity are placed together inside a chamber. The whole laser is then tuned by changing the index of refraction of the gas inside by varying its pressure.

The current trend with pulsed lasers is to use a very lossy, short oscillator cavity in which the longitudinal modes are nearly absent, making up for the cavity losses with a very high gain lasing medium. The front, output mirror of such a cavity may actually be *anti*reflection coated, with a reflectivity of only a percent or less.

Low gain, continuous wave (cw) lasers often use a combination of cavity length tuning along with dispersive element rotation, such as a prism or Lyot filter. Often, lasing on a traveling wave in a ring configuration is used to avoid longitudinal modes, as illustrated in Fig. 44.4. Some commonly used gain media are listed in Tables 44.1 and 44.2.

44.2.2 Pumping

Many methods, including electrical discharges and flashlamps, have been used to pump the gain media of lasers. Generally, the best pump is another laser.

Two notable pump lasers have dominated the field of tunable, visible lasers: pulsed neodymium YAG, frequency doubled to ≈ 503 nm, and cw Ar II ion at 514.5 nm. Both are extremely effective at exciting the highly efficient rhodamine class dyes in the red–yellow portion of the visible spectrum. The typical pump beam of a Nd/YAG laser enters the amplifying dye cell transversely along one on the faces of the cell. The typical cw pump beam enters the dye almost collinearly with the laser axis.

By temporarily *spoiling* the Q by making the laser cavity lossy, lasing can be held off until the gain medium stores a greater energy density than the minimum required for lasing. Rapidly switching off the loss mechanism releases this energy in one giant pulse. An electronic optical shutter, such as a Pockels cell, or a saturable dye inside the laser cavity, designed to photobleach from the spontaneous emission just before the laser reaches threshold, are commonly used.

Periodically spoiling the laser gain or the cavity Q at the period of a round trip produces intense, short pulses. Viewed from the frequency domain, the phases of individual longitudinal modes are *locked* together to produce a light packet circulating at the frequency of the reciprocal of the mode spacing. Extremely short pulses (< 1 ps) can be produced by mode locking. Practically, mode locking can be achieved by using a thin, saturable absorber near one of the cavity mirrors [6], or by acoustically modulating an optical element in the cavity – even an end mirror itself. One of the best ways of mode locking is to pump a short lifetime gain medium, such as a dye, with mode locked laser light, such as from a mode locked argon ion laser [7].

44.3 Interaction of Laser Light with Matter

44.3.1 Linear Absorption

The absorption cross section σ_{fi} for transition to the final state $|f\rangle$, when integrated over frequency ν, is given theoretically by the leading first-order perturbation of the initial

Table 44.1 Fixed frequency lasers

Laser	Wavelength (nm)	Excitation method
ArCl	≈170 (band)	Pulsed, gas discharge
ArF	≈193	Pulsed, gas discharge
KrCl	≈222	Pulsed, gas discharge
KrF	≈248	Pulsed, gas discharge
XeBr	≈282	Pulsed, gas discharge
XeCl	≈308	Pulsed, gas discharge
XeF	≈351, 353	Pulsed, gas discharge
N_2	≈337.1 (other bands)	Pulsed (1–10 ns), gas discharge
Ar^+	488.0, 514.5 (454.4, 457.9, 465.8, 472.7, 476.5, 501.7, 528.7)	cw, gas discharge
Ar^{+2}	351.1, 363.8	cw, gas discharge, high magnetic field
Kr^+	568.2, 647.1, (476.2, 520.8, 530.9)	cw, gas discharge
Kr^{+2}	350.7, 356.4, 406.7	cw, gas discharge, high magnetic field
Ne/He	632.8, 1152.3, 3390 (others)	cw, gas discharge
Cr^{+3}-Ruby	694.3	Pulsed, flashlamp
Nd^{+3}-YAG	≈1065, ≈1300	Pulsed: flashlamp; cw: lamp, LED or laser diode
Nd^{+3}-glass(various)	≈920, ≈1060, ≈1370	Pulsed, flashlamp
Yb^{+3}-glass	≈1060	Pulsed, flashlamp
Er^{+3}-glass(various)	≈1540, ≈1536, ≈1543, ≈1550	Pulsed: flashlamp; cw: lamp, LED or laser diode
Xe	3507	cw gas discharge
CO_2	≈10 600 (lines)	cw: gas discharge or gas dynamic
Molecular vibration and rotation	1×10^5–3×10^6 (numerous lines)	IR laser (CO_2, CO, ⋯)

Table 44.2 Approximate tuning ranges for tunable lasers

Laser	Wavelengths (nm)	Notes
Dye solution	<330 – >1200 [≈10 each dye]	Pulsed: laser, flashlamp; cw: laser
Alexandrite	700–820	Pulsed: lamp, laser; cw: laser
Ti^{+3}/Sapphire	680–1100	Pulsed: laser, lamp; cw: laser
GaAs	840–900	pn junction
InGaAlP/GaAs	630–700 [1–10]	pn junction
GaAsP	550–880	pn junction
AlGaAs, AlGaAs/GaAs	≈820 [1–20], 720–880	pn junction, temp. & current tuning
InP	≈900	pn junction, temp. & current tuning
GaInAs	906–3100	pn junction, temp. & current tuning
InGaAlAs/GaAs	800–1100	pn junction, temp. & current tuning
InPAs	900–4000 [1–50]	pn junction, temp. & current tuning
InGaAsP/InP	1200–1650	pn junction, temp. & current tuning
InAs	≈3100	pn junction, temp. & current tuning
InSb	≈5200	pn junction, temp. & current tuning
PbS	≈4300	pn junction, temp. & current tuning
PbTe	≈6500	pn junction, temp. & current tuning
PbSe	≈8500	pn junction, temp. & current tuning
PbSnSeTe “Lead Salt Diode”	4500–15,000 [1–50]	pn junction, temp. & current tuning
Color Centers: (F2+)/LiF	800–1040	cw: laser, Ar, Kr
/NaF	900–1050	cw: laser, Ar, Kr
/KCl:Tl	1400–1700	cw: laser, Ar, Kr, Nd/YAG
/KF	1300–1400	cw: laser, Ar, Kr, Nd/YAG
/NaCl	1400–1600	cw: laser, Ar, Kr, Nd/YAG
/KCl	1600–1700	cw: laser, Ar, Kr, Nd/YAG
/KBr	1700–1900	cw: laser, Ar, Kr, Nd/YAG
/KCl:Li	2500–2900	cw: laser, Ar, Kr, Nd/YAG
/KCl:Na	1600–1950	cw: laser, Ar, Kr, Nd/YAG

state $|i\rangle$ in the electric dipole approximation

$$\int \sigma_{fi}(\nu)\,\mathrm{d}\nu = 4\pi^2\alpha\bar{\nu}\left|\langle f|\sum_e \boldsymbol{r}_e\cdot\hat{\boldsymbol{\epsilon}}|i\rangle\right|^2 , \qquad (44.26)$$

where the sum is over all charges e at distances r_e, $\hat{\boldsymbol{\epsilon}}$ is a unit polarization vector, and $\bar{\nu}$ is the averaged transition energy. Averaged over orientations and summed over possible final states, each electron contributes to the total integrated absorption cross section one electron oscillator, $\pi r_0 c \approx 0.03\,\mathrm{cm^2\,s^{-1}}$; here, r_0 is the classical electron radius. Electronic absorption bands typically contain an oscillator strength $f = 0.01{-}0.5$ of an *electron oscillator*, while weaker vibrational transitions have $f = 10^{-6}{-}10^{-4}$ in each band.

For narrow lines with radiation of broader band width $\Delta\nu$ at flux density J, the linear absorption rate constant can be usefully estimated as $(\pi r_0 c) f J/\Delta\nu$.

44.3.2 Multiphoton Absorption

Second-order perturbation theory gives the theoretical two-photon contribution to the absorption. An absorption cross section $\sigma^{(2)}J_1$ for a photon of frequency ν_2 is induced by an off-resonance monochromatic field of frequency ν_1 and photon flux density J_1. When integrated over the frequency of the second photon, the second-order cross section can be related to the dipole matrix elements

$$\int \sigma^{(2)}_{fi}(\nu_1,\nu_2)J_1\,\mathrm{d}\nu_2 = \frac{4\pi^2\alpha^2}{\nu_1\bar{\nu}_2}J_1 \times\left|\sum_m \frac{\nu_{fm}\nu_{mi}\langle r_{fm}\rangle\langle r_{mi}\rangle}{\nu_{mi}-\nu_1}\right|^2 , \qquad (44.27)$$

where

$$\langle r_{fm}\rangle = \langle f|\sum_e \boldsymbol{r}_e\cdot\hat{\boldsymbol{\epsilon}}_2|m\rangle ,$$
$$\langle r_{mi}\rangle = \langle m|\sum_e \boldsymbol{r}_e\cdot\hat{\boldsymbol{\epsilon}}_1|i\rangle , \qquad (44.28)$$

and the sum is taken over intermediate states $|m\rangle$ having frequencies ν_{mi} and ν_{fm} for transitions to the initial and final states. The energy for the overall transition comes from two photons; hence the two-photon resonance condition $\nu_{fi} = \nu_1 + \nu_2$. A special case often occurs when only one radiation frequency is used: then $\nu_1 = \nu_2$, and two-photon resonance is achieved when the energy of the transition corresponds to twice the frequency of the radiation field.

This integrated, induced cross section is roughly of the order $\alpha(\pi c r_0)^2 J_1/(\nu_1\bar{\nu}_2)$. Two-photon absorption becomes comparable to the one-photon absorption with off-resonance fields on the order of

$$J_1 \approx \frac{\nu_1\nu_2}{\alpha\pi c r_0} , \qquad (44.29)$$

or about 10^{21} photons $\mathrm{s^{-1}\,cm^{-2}}$ ($10^{17}\,\mathrm{W\,m^{-2}\,s^{-1}}$ for typical green light).

Typical dipole-allowed molecular multiphoton absorption cross sections are $\approx 10^{-58}\,\mathrm{m^4\,s}$ for two photons and $10^{-94}\,\mathrm{m^6\,s^2}$ for three photons.

Multiphoton absorption was one of the first effects explored with lasers. Two-photon absorption was first reported for inorganic crystals containing europium ions [8]. Blue and ultraviolet fluorescence appeared in the interaction of red ruby laser light with organic compounds [9–12]. Others observed two-photon absorption directly [13, 14]. Selection rules for multiphoton absorption are summarized by *McClain* [15]; recent work is reviewed by *Ashfold* and *Howe* [16].

Highly excited states may subsequently ionize in the intense fields in a multiphoton ionization (MPI) process. The ionization signal is often detected in a proportional ionization cell. A low pressure cell containing the vapor of a transition metal organometallic, such as iron carbonyl or ferrocene which photodissociates to give the metal atom, may be used for wavelength calibration by MPI.

44.3.3 Level Shifts

High radiation power causes resonant frequencies to shift, responding to the ac Stark effect [17, 18]. Even moderate fields, tuned near resonance, interact strongly with an atom or small molecule, which undergoes rapid excitation and stimulated emission at the characteristic power dependent Rabi frequency,

$$\nu_{\mathrm{Rabi}} = \frac{2\pi g_1}{g_1+g_2}\sigma_{21}J . \qquad (44.30)$$

Fluorescence from such an interacting system has a characteristic *head and shoulders* spectrum best understood as radiation at the fundamental frequency amplitude modulated at the Rabi frequency [19].

44.3.4 Hole Burning

Radiation at a particular frequency generally moves population out of states that absorb that radiation. Molecules that interact resonantly with the radiation may also spontaneously emit at different frequencies, thereby ending in nonabsorbing states. This optical pumping effect can make resonance

features in an absorption spectrum disappear at high power levels [20]. Depletion may appear as a *hole* in the absorption spectrum [21]. Recently, interest has shifted to permanent *hole burning* as a method of information storage in materials.

Hole burning is the basis for Doppler-free Lamb-dip spectroscopy, in which only absorbing atoms or molecules having little or no velocity component along the axis of two counterpropagating beams are temporarily depleted [22]. This technique is commonly used for laser frequency stabilization, such as with the iodine-locked He–Ne laser.

44.3.5 Nonlinear Optics

Multiplying

Nonlinear susceptibility of an optical medium can generate radiation at frequencies which are multiples of the frequency of laser radiation passing through. Phenomenologically, the second order polarization

$$\boldsymbol{P}_{2\nu} = \epsilon_0 \chi^{[2]} \boldsymbol{E}_{\nu}^2 \tag{44.31}$$

is given in terms of the second order nonlinear susceptibility $\chi^{[2]}$, a third rank tensor, and the electric field at the fundamental frequency (see Chap. 76). This nonlinear susceptibility can range from 0.5−5 pm/V for typical materials used for frequency doubling. Typical materials and their use are reviewed by *Bordui* and *Fejer* [23].

For a nonlinear process occurring over a length l in a cylindrical region with Gaussian waist w_0 with polarization P_0 on axis, the far field flux is given by

$$J(R,\theta) = \frac{\pi^4 \nu^3 n^3 w_0^4 P_0^2}{4hc^3 \epsilon_0 R^2} \left(\frac{\sin^2[(k_0 - k\cos\theta)l/2]}{(k_0 - k\cos\theta)^2} \right) \times \exp\left[-k^2 w_0^2 \sin^2(\theta)/2\right] . \tag{44.32}$$

Here, n is the index of refraction and k the propagation constant for the induced radiation, while k_0 is that for the induced polarization, the vector sum of those of the original radiation. When phase matched, $k_0 - k\cos\theta = 0$, and the term in the brackets maximizes to $(l/2)^2$.

The greatest difficulty is in selecting materials which can be phase matched such that the relative phases of the fundamental and overtone radiation propagate together through the material; otherwise radiation at the higher frequency generated at different places inside the material destructively interfere. Phase matching is usually achieved by either angle tuning of a birefringent crystal, or by temperature tuning.

Only materials without a center of inversion in their crystal structures have a second order nonlinear susceptibility. All materials, including gases, will have a third order nonlinear susceptibility $\chi^{[3]}$. This can be used to generate third harmonics, especially in the vacuum ultraviolet (VUV), where doubling materials are not available [24, 25].

Mixing

The same materials that permit frequency doubling and tripling also allow 3-wave and 4-wave frequency mixing. The frequency matching conditions are, respectively,

$$\begin{aligned} \nu_1 \pm \nu_2 &= \nu_3 , \\ \nu_1 \pm \nu_2 \pm \nu_3 &= \nu_4 . \end{aligned} \tag{44.33}$$

Tunable UV radiation may be generated by adding the frequencies of a fixed and tunable visible outputs. Tunable IR has been obtained by differencing fixed and tunable visible lasers. Mixing of radiation from an Ar ion laser with that from a tuned R6G dye laser in lithium iodate to produce tunable 2200−4600 nm radiation is noteworthy.

Optical Parametric Oscillator

It is possible to reverse 3-wave mixing, generating two frequencies whose sum is that of the input radiation. In parametric generation, the output frequencies are given by the phase match conditions. Both the desired frequency and the secondary *idler* frequency must be allowed to build up in the nonlinear medium. The idler radiation is not present initially, but results from the frequency mixing process itself. The process has many of the characteristics of a laser oscillator, including that of a gain threshold. This makes tuning of an optical parametric oscillator similar to that of a laser, but with more degrees of freedom: now oscillation at two frequencies must be attained simultaneously, along with the correct *phase matching* of the nonlinear material [26].

44.3.6 Raman Scattering

It is possible to have one or more of the fields in a mixing process belong to just polarization, rather than radiation. The frequency additive case of multiphoton absorption has already been considered; the frequency subtractive case is Raman scattering.

Incoherent Raman Scattering

Radiation at a higher frequency can excite a lower frequency vibration or rotation within a material, with appearance of radiation at the frequency of the incident radiation minus that of the absorption. The integrated cross section for this effect is given by Eq. (44.27). However, in this case the cross section is for *emission* of the second photon. The rate of spontaneous Raman emission is obtained by multiplying Eq. (44.27) by the spectral flux density of the zero-point field, $8\pi\nu^2/\epsilon_r c$. Typical vibrational Raman cross sections for

transparent molecules are about $10^{-34}\,m^2\,sr^{-1}$ in the blue–green (488 nm) [27].

Alternatively, energy can be extracted from an excited state, with the inelastically scattered photon departing with the sum of the incident frequency and that of the deexcitation. The term *anti-Stokes* distinguishes it from the more usual *Stokes* type of Raman scattering.

Coherent Raman Emission

The integrated cross section for emission stimulated at the Raman frequency is given directly by Eq. (44.27).

A fourth-order mixing process that is less susceptible to saturation involves coherent anti-Stokes Raman scattering (CARS). Two beams excite the material: the difference of their frequencies corresponds to an excitation of the material. Stimulated Raman scattering excites the material, which then deexcites through an anti-Stokes process, giving rise to a third, higher frequency radiation field. The phase is determinate, and the radiation leaves the region of scattering as a beam [28].

If the incident radiation induces a Raman process over a sufficiently long path, the stimulated Raman process can be used for gain at both the Stokes and anti-Stokes frequencies. Since spontaneous Raman processes are proportional to the integrated cross section, while gain in the stimulated Raman process is proportional to the peak cross section, simple materials with sharp, simple line spectra are most suitable for Raman gain media. While Raman lasers have been produced using vibrational excitation of organic liquids, currently the most important technical application is for Raman shifting the output of lasers, tunable or otherwise, to frequencies which otherwise would be inaccessible. The high pressure H_2 Raman shifter produces, at low powers, beams consisting almost entirely of well separated, sharp lines shifted by $4160\,cm^{-1}$ from the pump beam; at high powers, a series of Stokes and anti-Stokes bands appear, each separated by $4160\,cm^{-1}$ from each other.

44.4 Recent Developments

One of the most exciting advancements in the past decade in laser physics has been the generation of optical frequency combs; and, more specifically, their applicability in the domain of high-resolution laser spectroscopy. Basically, through a superposition process of many continuous wave modes, a short train of frequency spikes may be produced from a mode-locked laser [29] (see also Sect. 30.1.5). These spikes are equally spaced and are referred to as a frequency comb. The frequency ω_n of the n-th cavity mode may be expressed as

$$\omega_n = n\omega_r + \omega' , \tag{44.34}$$

where ω_r is characteristic of the laser and ω' is a frequency offset due to the difference between the phase and group velocity of the superposed waves.

The microwave frequencies ω_r and ω' are determined through the use of nonlinear optics. Once these two parameters are determined, any unknown optical frequency ω_o may be measured by recording the beat frequency between it and the closest comb frequency. This technique gives experimenters a high-precision method for the spectroscopic determination of such fundamental quantities as the fine structure constant, the Rydberg constant, and the Lamb shift [30, 31].

Acknowledgment Text and references updated by Mark M. Cassar.

References

1. Einstein, A.: Phys. Z. **18**, 121 (1917)
2. Kogelnik, H., Li, T.: Proc. IEEE **54**, 1312 (1966)
3. Verdeyen, J.T.: Laser Electronics, 3rd edn. Prentice Hall, Englewood Cliffs (1994)
4. Svelto, O.: Principles of Lasers. Plenum, New York (1976)
5. Wallenstein, R., Hänsch, T.W.: Opt. Commun. **14**, 353 (1975)
6. Ippen, E.P., Shank, C.V., Dienes, A.: Appl. Phys. Lett. **21**, 348 (1972)
7. Jain, R.K., Ausschnitt, C.P.: Opt. Lett. **2**, 117 (1978)
8. Kaiser, W., Garrett, C.G.B.: Phys. Rev. Lett. **7**, 229 (1961)
9. Peticolas, W.L., Goldsborough, J.P., Rieckhoff, K.E.: Phys. Rev. Lett. **10**, 4345 (1963)
10. Peticolas, W.L., Reickhoff, K.E.: J. Chem. Phys. **39**, 1347 (1963)
11. Singh, S., Stoicheff, B.P.: J. Chem. Phys. **38**, 2032 (1963)
12. Weisz, S.Z., Zahlen, A.B., Gilreath, J., Jarnagin, R.C., Silver, M.: J. Chem. Phys. **41**, 3491 (1964)
13. Hopfield, J.J., Warlock, J.M., Park, K.: Phys. Rev. Lett. **11**, 414 (1963)
14. Staginnus, B., Frölich, D., Caps, T.: Rev. Sci. Instrum. **39**, 1129 (1968)
15. McClain, W.M.: Acc. Chem. Res. **7**, 129 (1974)
16. Ashfold, M.N., Howe, J.D.: Annu. Rev. Phys. Chem. **45**, 57 (1994)
17. Carmichael, H.J., Walls, D.F.: J. Phys. B **9**, 1199 (1976)
18. Li, L.-P., Yang, B.-X., Johnson, P.M.: J. Opt. Soc. Am. **2**, 748 (1985)
19. Mallow, B.R.: Phys. Rev. **188**, 1969 (1969)
20. Rothberg, L.J., Gerrity, D.P., Vaida, V.: J. Chem. Phys. **75**, 4403 (1981)
21. Völker, S.: Annu. Rev. Phys. Chem. **40**, 499 (1989)
22. Bennett Jr., W.R.: Phys. Rev. **126**, 580 (1962)
23. Bordui, P.F., Fejer, M.M.: Annu. Rev. Mater. Sci. **23**, 321 (1993)
24. Kung, A.: Opt. Lett. **8**, 24 (1983)
25. Bokor, J., Bucksbaum, P., Freeman, R.: Opt. Lett. **8**, 217 (1983)
26. Falk, J., Yarbourough, J.M., Ammann, E.O.: IEEE J. Quantum Elec. **7**, 359 (1971)
27. Penney, C.M., St. Peters, R.L., Lapp, M.: J. Opt. Soc. Am. **64**, 712 (1974)
28. Regnier, P.R., Taran, J.P.: Appl. Phys. Lett. **23**, 240 (1973)
29. Udem, T., Holzwarth, R., Zimmerman, M., Goble, C., Hänsch, T.: Top. Appl. Phys. **95**, 295 (2004)
30. Hensley, J.M.: A precision measurement of the fine structure constant. Ph.D. Thesis. University, Stanford, Stanford (2001)
31. de Beauvoir, B., Schwob, C., Acef, O., Jozefowski, L., Hilico, L., Nez, F., Julien, L., Clairon, A.: Eur. Phys. J. D **12**, 61 (2000)